

***Arabidopsis* Proline Dehydrogenase Contributes to Flagellin-Mediated PAMP-Triggered Immunity by Affecting RBOHD**

Georgina Fabro, Yanina Soledad Rizzi, and María Elena Alvarez

Centro de Investigaciones en Química Biológica de Córdoba, CIQUIBIC, CONICET, Departamento de Química Biológica, Facultad de Ciencias Químicas, Universidad Nacional de Córdoba, Ciudad Universitaria, X5000HUA Córdoba, Argentina

Accepted 30 May 2016.

Plants activate different defense systems to counteract the attack of microbial pathogens. Among them, the recognition of conserved microbial- or pathogen-associated molecular patterns (MAMPs or PAMPs) by pattern-recognition receptors stimulates MAMP- or PAMP-triggered immunity (PTI). In recent years, the elicitors, receptors, and signaling pathways leading to PTI have been extensively studied. However, the contribution of organelles to this program deserves further characterization. Here, we studied how processes altering the mitochondrial electron transport chain (mETC) influence PTI establishment. With particular emphasis, we evaluated the effect of proline dehydrogenase (ProDH), an enzyme that can load electrons into the mETC and regulate the cellular redox state. We found that mETC uncouplers (antimycin or rotenone) and manganese superoxide dismutase deficiency impair flg22-induced responses such as accumulation of reactive oxygen species (ROS) and bacterial growth limitation. ProDH mutants also reduce these defenses, decreasing callose deposition as well. Using ProDH inhibitors and ProDH inducers (exogenous Pro treatment), we showed that this enzyme modulates the generation of ROS by the plasma membrane respiratory burst NADPH oxidase homolog D. In this way, we contribute to the understanding of mitochondrial activities influencing early and late PTI responses and the coordination of the redox-associated mitochondrial enzyme ProDH with defense events initiated at the plasma membrane.

Plants make use of a surveillance system to detect microbe- or pathogen-associated molecular patterns (MAMPs or PAMPs) in potential invaders. This system includes surface-localized pattern recognition receptors (PRRs) that stimulate MAMP- or PAMP-triggered immunity (PTI) and, therefore, control non-adapted pathogens without compromising cell viability (Nicaise et al. 2009). The PTI pathway activated by bacterial flagellin is well characterized in *Arabidopsis*. It becomes stimulated by binding of flagellin or its derived peptide, flg22, to the PRR FLS2. This event initiates a complex signaling transduction network including successive phosphorylation steps that target FLS2, its coreceptor BIK1, and the Ca²⁺-sensitive respiratory burst NADPH oxidase homolog D (RBOHD), responsible for

generation of apoplastic reactive oxygen species (aROS) (Kadota et al. 2015). RBOHD activation signals early and late PTI responses, such as stomatal closure and callose deposition at the cell wall, respectively (Galletti et al. 2008; Mersmann et al. 2010). In addition, the FLS2 pathway involves a mitogen-activated protein kinase cascade that triggers large gene expression changes, to induce flg22-responsive kinase 1 (*FRK1*), *WRKY29* transcription factor, and other genes (Asai et al. 2002; Pandey and Somssich 2009).

RBOHD also operates in effector-triggered immunity (ETI), a second layer of defenses based on detection of pathogen effectors by intracellular plant resistance (R) proteins. In this case, the pathway leads to cell death causing a hypersensitive response (HR) that is induced by Ca²⁺ influx, aROS burst, salicylic acid (SA), and nitric oxide (NO) accumulation (Mur et al. 2008; Tsuda and Katagiri 2010). During defense activation, intracellular redox changes derived from ROS production at chloroplasts, mitochondria, and peroxisomes influence the activity of plasma membrane NADPH oxidases (Chaouch et al. 2012; Shapiguzov et al. 2012; Yao and Greenberg 2006). However, the components that support mitochondrial ROS (mtROS) burst and the interregulation of this response with RBOHD activation are mostly unknown.

Under ETI or cell death-inducing conditions, SA, NO, or bacterial toxins alter mitochondrial traits by modifying respiration, membrane potential, or mtROS content (Krause and Durner 2004; Lam et al. 2001; Mur et al. 2008; Xie and Chen 1999; Zhang and Xing 2008). SA uncouples electron flow in the mitochondrial electron transport chain (mETC) MTI or ATP synthesis during HR (Norman et al. 2004; Xie and Chen 2000). *Nicotiana tabacum* cells trigger fast mitochondrial O₂⁻ accumulation in response to *Pseudomonas syringae* pv. *maculicola* (Cvetkovska and Vanlerbergh 2012), whereas *Arabidopsis* cells accumulate mtROS after treatment with *Pseudomonas syringae* harpin Z (Krause and Durner 2004). In the latter case, mtROS burst is associated with reduction in ATP levels, suggesting it arises from imbalances in the mETC. Likewise, the death-inducing agent protoporphyrin IX triggers a rapid (1.5 h) mtROS burst in *Arabidopsis* (Yao and Greenberg 2006). Besides these findings, mitochondria also influence defenses that are not accompanied by cell death. Reduction in the amount of the catalytic subunit of complex II (succinate dehydrogenase) inhibits production of H₂O₂ at this organelle, increasing susceptibility to *Rhizoctonia solani* and *P. syringae* pv. *tomato* DC3000 (Gleason et al. 2011). Decrease in the outer mitochondrial membrane protein AAA-type ATPase AtOM66 impairs defense-gene activation generating susceptibility to *P. syringae* pv. *tomato* (Zhang et al. 2014). Conversely, plants overexpressing AtOM66 and mutants in the mitochondrial inner-membrane import motor AtPAM16 enhance

Corresponding author: M. E. Alvarez; E-mail: malena@fcq.unc.edu.ar

*The e-Xtra logo stands for “electronic extra” and indicates that three supplementary figures and one supplementary table are published online.

resistance to virulent *P. syringae* pv. *maculicola*. Indeed, AtPAM16 seems to act as a negative regulator of mtROS production (Huang et al. 2013).

A well-known metabolic pathway that takes place at the inner mitochondrial membrane and affects pathogen defenses is the one involving the transformation of proline (Pro) into glutamic acid. Pro dehydrogenase (ProDH; EC 1.5.5.2, formerly 1.5.99.8) catalyzes the rate-limiting step of this pathway by converting Pro into pyrroline-5-carboxylate (P5C) with generation of FADH₂. Subsequently, P5C is nonenzymatically transformed into glutamate semialdehyde that is oxidized to glutamate by Δ^1 -pyrroline-5-carboxylate dehydrogenase (P5CDH) producing NADH (Elthon and Stewart 1981). ProDH can load electrons into the mETC (Schertl et al. 2014), and this capacity seems to be exacerbated during abiotic stress, when the enzyme participates in the Pro/P5C cycle (Miller et al. 2009). In this case, hyperactivation of ProDH increases the chance to transfer electrons to O₂ and, therefore, generate mtROS (Ben Rejeb et al. 2014). Interestingly, ProDH also potentiates general ROS burst in tissues triggering HR (Cecchini et al. 2009, 2011a; Senthil-Kumar and Mysore 2012). In this case, the enzyme may also function in the Pro/P5C cycle (Monteoliva et al. 2014), but localization of ROS has not been evaluated. Even more, the effect of ProDH in RBOHD-derived aROS generation remains to be analyzed.

In this work, we analyzed how flg22-induced PTI is altered by mitochondrial dysfunctions, using three different experimental models, including wild-type tissues treated with mETC inhibitors, manganese superoxide dismutase (MnSOD)-deficient plants, and ProDH mutants. Our results indicate that PTI is sensitive to mETC uncoupling and requires ProDH for optimal generation of aROS by RBOHD.

RESULTS

mETC alterations reduce PTI responses.

We analyzed hallmarks of PTI induced by flg22 (100 nM) in three experimental models impaired in mitochondrial functions: i) wild-type plants treated with mETC inhibitors, ii) mutant or silenced MnSOD plants; and iii) ProDH mutants.

Antimycin A (AA) and rotenone (Rtn) were used as mETC inhibitors, as they block complex III electron transport between cytochromes b and c or complex I between mitochondrial NADPH oxidase and ubiquinone, respectively (Møller 2001). AA (10 μ M) and Rtn (40 μ M) triggered mtROS accumulation from 30 min posttreatment, as indicated by colocalization of signals from the mitochondrial marker Mitotracker orange and the ROS-sensitive probe CM-H₂DCFDA (Supplementary Fig. 1A). As expected, both treatments activated the *alternative oxidase 1a* gene (*AOX1a*, At3g22370), but neither of them caused cell death. Then, AA and Rtn were used at these concentrations in the subsequent studies.

AA and Rtn induced *FRK1* and *WRKY29* expression (Fig. 1A), suggesting they affect flg22-sensitive defenses. To better assess their influence on this pathway, we exposed leaf discs to AA or Rtn and, 30 min later (when mtROS was established), we treated them with flg22 to monitor aROS. We used a luminol-based ROS assay for this purpose (Gómez-Gómez et al. 1999). Samples pretreated with the inhibitors accumulated less aROS than mock-pretreated samples, with differences of 30 to 35% (Fig. 1B). To test if Rtn or AA altered the capacity of Col-0 plants to restrict nonadapted pathogen growth, we treated the leaves with these compounds and, 4 h later, sprayed them with *P. syringae* pv. *tomato* Δ *hrcC*. This bacterial strain grows poorly in Col-0, since it does not deliver effectors that counteract PTI (Zipfel et al. 2004). The *P. syringae* pv. *tomato*- Δ *hrcC* content was five times greater in plants treated with AA and Rtn, and this was sustained over 3 days (Fig. 1C). Therefore, PTI is impaired in tissues that increase mtROS by blocking the electron flow in complex III or complex I.

As a second model for mitochondrial dysfunction, we used plants deficient in mitochondrial MnSOD. This enzyme converts O₂⁻ generated as a byproduct of mETC into H₂O₂ (Møller 2001), and its decrease causes mitochondrial matrix oxidation and abnormal respiration (Morgan et al. 2008). We first evaluated flg22-triggered aROS accumulation in MnSOD insertional mutants (heterozygous lines HT 1 to 11) and MnSOD silenced (AS7) plants. We used a pool of heterozygous seeds, since these mutants generated a range of defects in the female gametophyte (Martin et al. 2013). flg22-mediated aROS was analyzed on 11 independent mutants and ROS reduction was detected in seven of them, indicating variability in this response (Fig. 1D, top). When the 11 mutant plants were evaluated in bulk, they showed significant ROS reduction, as AS7 plants did (Fig. 1D, bottom). In addition, the MnSOD mutants were less efficient than Col-0 plants to control *P. syringae* pv. *tomato*- Δ *hrcC* proliferation at 3 days posttreatment (Fig. 1E). These results indicated that impairment of O₂⁻ scavenging negatively affects PTI.

We next evaluated PTI phenotypes in ProDH mutants. *Arabidopsis* contains two active enzyme isoforms encoded by *AtProDH1* (At3g30775) and *AtProDH2* (At5g38710) genes (Funck et al. 2010; Kiyosue et al. 1996). Our efforts to generate full *ProDH* silenced plants were unsuccessful, since T1 lines were unable to set seeds (Cecchini et al. 2011a). As null *prodh1/2* double mutants have not been reported, we used the available single mutant plants *prodh1-3*, *prodh1-4*, and *prodh2-2* (Col-0 background), and *prodh2-1* (Ler ecotype) (Funck et al. 2010). Clearly, *prodh1-3*, *prodh2-2* (Fig. 2A), and all other mutants (Fig. 2B) reduced aROS accumulation in response to flg22 (50 to 60% regarding wild-type plants) by altering the intensity but not kinetics of this response (Fig. 2A). Given that single mutants showed similar phenotypes (Fig. 2B), we conducted the following studies in *prodh1-3* and *prodh2-2*, which share the same genetic background.

As late PTI markers, we monitored callose deposition at the cell wall and pathogen growth restriction. In response to flg22 or *P. syringae* pv. *tomato*- Δ *hrcC*, the *prodh1-3* and *prodh2-2* mutants generated far fewer callose deposits than Col-0 plants (70% reduction) (Fig. 2C). In addition, these mutants displayed increased susceptibility to *P. syringae* pv. *tomato*- Δ *hrcC*, as they contained higher doses of pathogen than control plants (eight to 10 times by day 3) (Fig. 2D). However, *prodh1-3* and *prodh2-2* did not alter the activation of *FRK1* and *WRKY29* by flg22 (Fig. 2E). Thus, ProDH clearly affects flg22-induced aROS burst and resistance to *P. syringae* pv. *tomato*- Δ *hrcC* but not *FRK1* and *WRKY29* activation.

ProDH mutants are not affected in *FLS2* and *RBOHD* gene expression.

Some *Arabidopsis* plants with reduced responses to flg22 have low expression of *FLS2* (Boutrot et al. 2010; Cecchini et al. 2015; Yi et al. 2014) or *RBOHD* (Daudi et al. 2012; Monaghan et al. 2014; Stegmann et al. 2012). We wondered if this occurred in the *prodh* mutants. To test this, we quantified *FLS2* and *RBOHD* transcripts in *prodh1-3* and *prodh2-2* plants. As shown in Figure 3, the *prodh* mutants did not reduce the expression of these genes, rather showing a nonsignificant activation of *FLS2* (*prodh2-2*) or both genes (*prodh1-3*). This indicates that attenuation of their flg22-induced responses would not result from subnormal levels of the peptide receptor or the enzyme that generates aROS.

ProDH activity supports generation of aROS by flg22.

To evaluate if ProDH affects PTI by acting as an enzyme, we assessed the effect of ProDH inhibitors on flg22-mediated aROS burst. The nonreducing Pro analog T4C (thiazolidine-4-carboxylate) inhibits *Arabidopsis* ProDH activity at 1 mM, as determined by consumption of radiolabeled Pro on leaf tissues

(Monteoliva et al. 2014; Rizzi et al. 2015). In turn, THFA (L-tetrahydro-2-furoic acid) exerts this effect in the range of 1 to 5 mM (Krishnan et al. 2008; White et al. 2007). Interestingly, preincubation (2 h) of Col-0 samples with T4C or THFA decreased flg22-induced aROS burst in a dose-dependent manner (0.25 to 5.00 mM range). The ability of both compounds to inhibit ProDH throughout this range (Elthon and Stewart 1984; Miller et al. 2009; Monteoliva et al. 2014; Rizzi et al. 2015; Zhu et al. 2002) suggests that this enzyme activity is required for full aROS burst. Moreover, 2 mM T4C or 5 mM THFA reduced the aROS to 50% (Supplementary Fig. 2A) without affecting either ProDH

content or cell viability, and these compounds did not generate cell death at concentrations up to 20 mM (T4C) or 50 mM (THFA).

T4C and THFA reduced the intensity but not kinetics of aROS accumulation induced by flg22 (Fig. 4A), resembling the effect of ProDH mutations (Fig. 2A). Perception of flg22 by FLS2 was not altered by T4C or THFA, since preincubation of the peptide with inhibitors did not affect its capacity to increase aROS (Fig. 4B). In addition, T4C reduced by 50% the aROS content of *prodh1-3* and *prodh2-2*, indicating that both mutants have residual ProDH activity and both enzyme isoforms are required for full aROS burst (Fig. 4C).

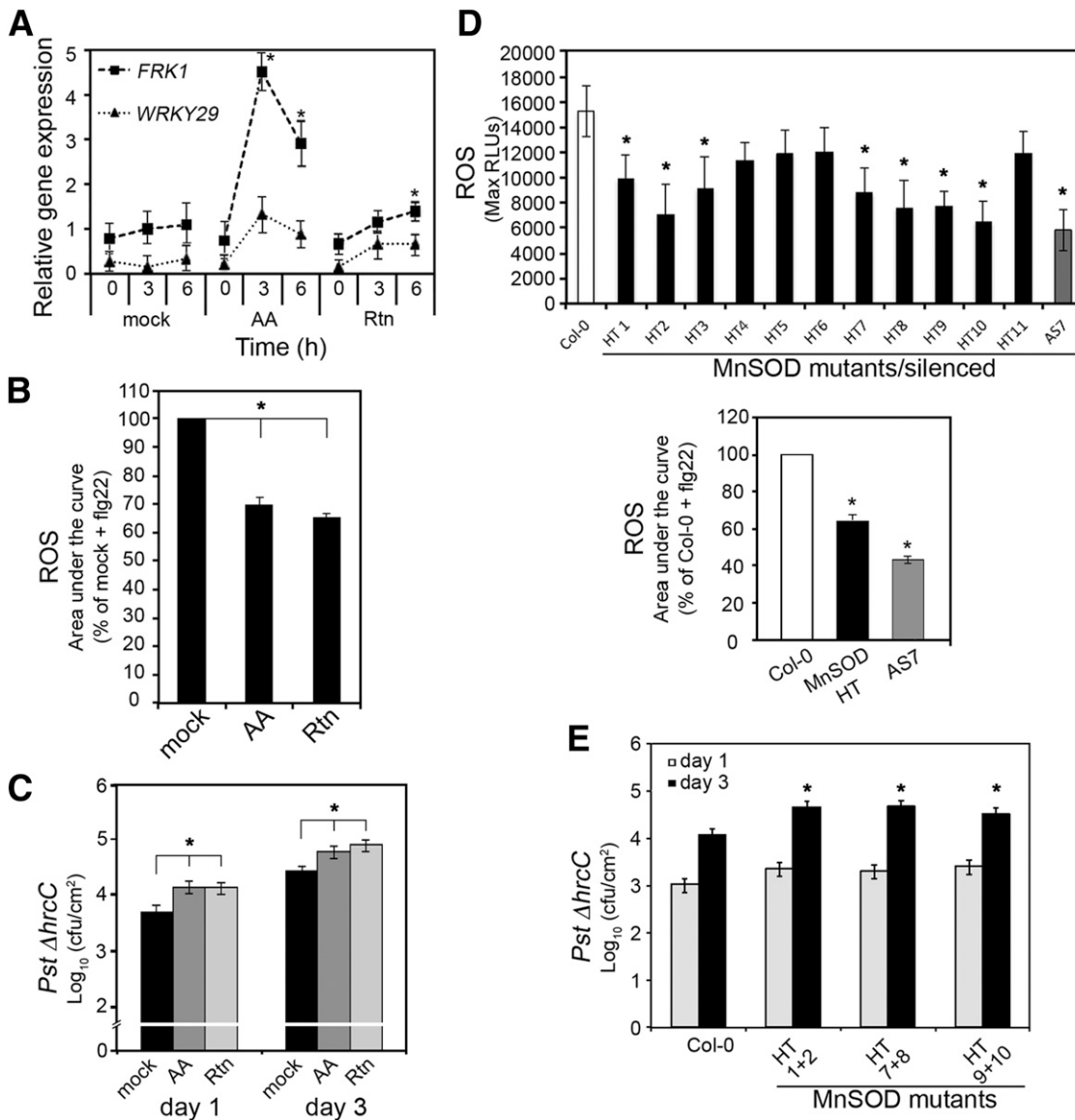


Fig. 1. Mitochondrial electron transport chain alterations affect pathogen-associated molecular pattern-triggered immunity responses. **A**, Expression of *FRK1* and *WRKY29* in response to mock (0.01% ethanol), antimycin A (AA) (10 μ M), or rotenone (Rtn) (40 μ M) treatments. Gene expression (mean \pm standard error [SE]) of three biological replicates) was determined by quantitative polymerase chain reaction (qPCR) regarding *UBQ5*, using the Pfaffl method. Asterisks (*) indicate significant differences to the control sample (0 h) of each treatment (analysis of variance, Tukey test, $P < 0.05$). **B**, Apoplastic reactive oxygen species (ROS) levels induced by flg22 in Col-0 leaf discs preincubated for 30 min with AA (10 μ M), Rtn (40 μ M), or mock solution. Areas under the curves are expressed as percentage of mock + flg22 treated plants. Three biological replicates (24 leaf discs each) were averaged. Asterisks (*) indicate significant differences (Z test) at $P < 0.01$. **C**, Col-0 plants were pretreated with mock solution, AA, or Rtn and were sprayed 4 h later with *P. syringae* pv. *tomato-ΔhrcC* (optical density at 600 nm [OD₆₀₀] = 0.01). Pathogen content was determined at the indicated times. Values correspond to mean \pm SE (four pools of three discs each). Asterisks (*) indicate significant differences regarding mock control according to *t* test ($P < 0.05$). One representative experiment of three biological replicates is shown. **D**, Top, maximum levels of flg22-induced apoplastic ROS expressed as relative luminescence units (RLUs) in Col-0 plants, manganese superoxide dismutase (MnSOD) mutants (HT1 to HT11), and MnSOD-silenced plants (AS7) (seven leaf discs per plant). Bottom, values (mean \pm SE) of area under the curve for samples shown in top (MnSOD heterozygous lines were averaged). Asterisks (*) indicate significant differences to Col-0 (Z test, $P < 0.05$). **E**, *P. syringae* pv. *tomato-ΔhrcC* growth in MnSOD mutant plants. Two heterozygous mutants were pooled and inoculated with OD₆₀₀ = 0.01. Values are mean \pm SE of four pools of three discs each. Asterisks (*) indicate statistically significant differences regarding Col-0 at day 3 (*t* test; $P < 0.05$).

Exogenous Pro potentiates the increase in aROS induced by flg22.

In *Arabidopsis*, the expression of *ProDH* can be induced by application of exogenous Pro (Kiyosue et al. 1996; Rizzi et al. 2015). In fact, Col-0 leaf discs treated with 1 mM Pro accumulated *AtProDH1* and *AtProDH2* transcripts and ProDH protein within 2 h (Fig. 5A). When Col-0 samples were exposed to 1 mM Pro (2 h) prior to addition of flg22, the aROS levels were enhanced (1.5 times regarding samples without Pro) (Fig. 5B). Importantly, if Col-0 leaf discs were incubated with Pro (1 mM, 2 h) but not with flg22, aROS were not detected (Fig. 5B). Thus, Pro did not increase aROS by itself but potentiated the flg22-triggered burst, probably by activating ProDH. In addition, samples floated for 2 h in up to 10 mM Pro did not manifest cell death signs.

Next, we preincubated *prodh1-3* and *prodh2-2* leaf discs with 1 mM Pro for 2 h and observed a marginal aROS increase in *prodh2-2*, with no differences in *prodh1-3* (Fig. 5B). This suggests that exogenous Pro has more impact on ProDH1 than

on ProDH2. Additionally, after Pro treatment, the mutants did not reach the aROS levels achieved in wild-type plants treated with flg22, suggesting that both isoforms are required for the full potentiation of aROS by Pro (Fig. 5B).

Finally, we examined whether potentiation of flg22-triggered aROS burst by Pro was dependent on RBOHD. For this, we monitored aROS on *rbohD* mutant samples exposed to Pro. As expected, flg22 did not increase aROS in this mutant (Fig. 5C). Interestingly, preincubation with Pro (1 mM, 2 h) did not generate aROS by flg22 in this plant, suggesting that potentiation of aROS by exogenous Pro mainly targets RBOHD activity. However, further studies will be required to elucidate how Pro and ProDH contribute to such effect.

DISCUSSION

This work analyzes how mitochondrial dysfunctions influence PTI. We found that AA and Rtn interfered with RBOHD-dependent

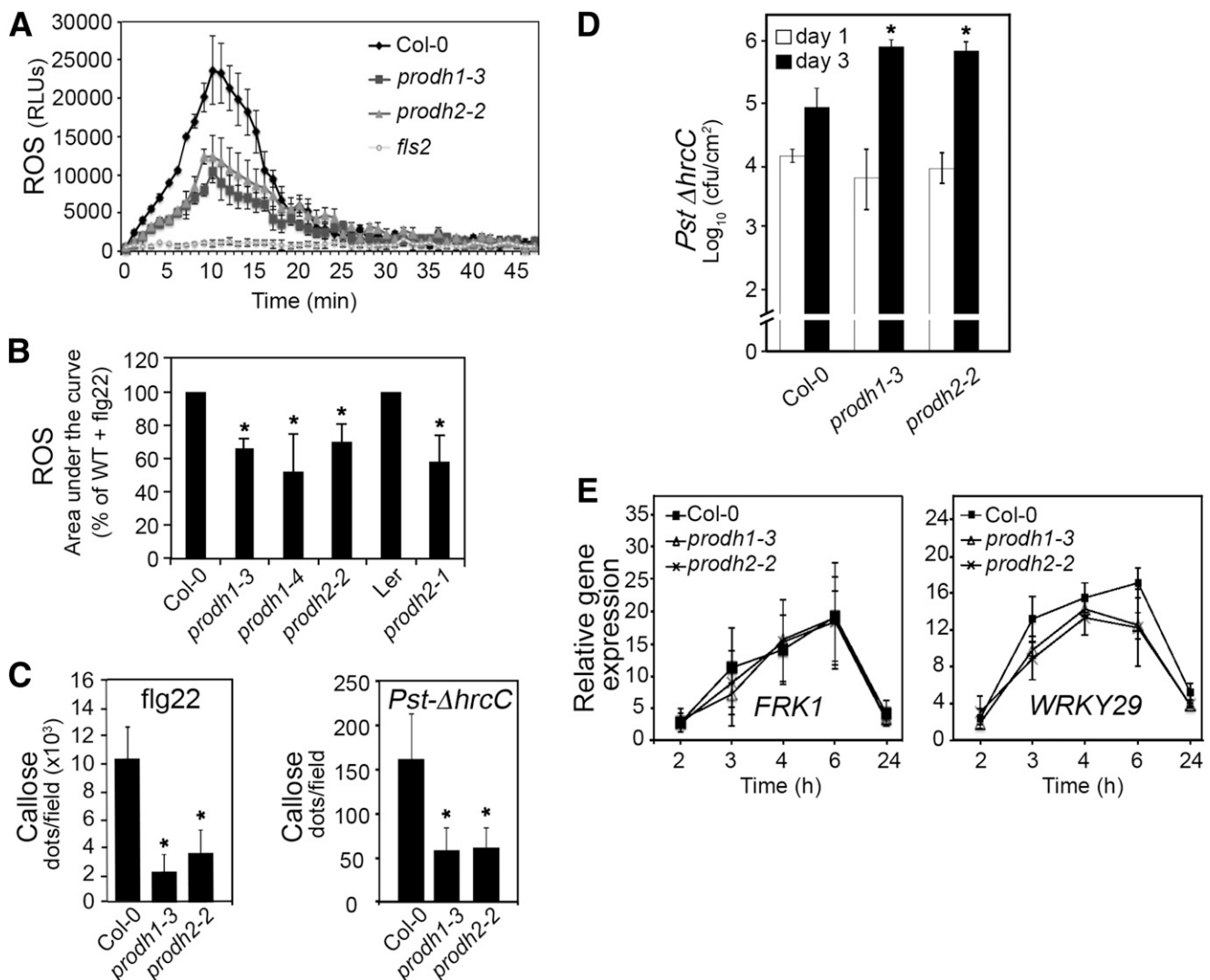


Fig. 2. *AtProDH1* and *AtProDH2* contribute to pathogen-associated molecular pattern-triggered immunity. **A**, Kinetics of flg22-induced apoplastic reactive oxygen species (aROS) burst in Col-0, *prodh1-3*, and *prodh2-2* plants. Values correspond to mean \pm standard error (SE) (24 leaf discs). The *fls2* mutant is used as negative control. **B**, flg22-mediated aROS levels in proline dehydrogenase (ProDH) single mutants expressed as percentage of values of elicited wild-type plants. Data are average of three independent experiments (mean \pm SE; 24 leaf discs each). Asterisks (*) indicate significant differences to wild-type plants (Z test $P < 0.05$). **C**, Callose deposition in Col-0, *prodh1-3*, and *prodh2-2* plants induced by flg22 or *P. syringae* pv. *tomato-ΔhrcC*. Values represent the quantitation of 20 fields per genotype. Asterisks (*) indicate significant differences to Col-0 (t test, $P < 0.01$). **D**, *P. syringae* pv. *tomato-ΔhrcC* content in single ProDH mutants. Plants were sprayed with bacterial suspensions at optical density at 600 nm = 0.05. Values are mean \pm SE (four pools of three discs each). Asterisks (*) indicate significant differences to Col-0 (t test, $P < 0.05$). **E**, Time course expression (quantitative polymerase chain reaction) of *FRK1* and *WRKY29* in flg22-treated Col-0, *prodh1-3*, and *prodh2-2* plants. Values (mean \pm SE from three biological replicates) are related to *UBQ5* expression, using the Pfaffl method. For C and D, similar results were obtained in three biological assays.

responses activated by flg22 (Fig. 1A, B, and C). This would be caused by blockage of mETC, as expected, and not by a direct effect on RBOHD, since these inhibitors do not affect plant NAD(P)H oxidases directly (Brightman and Morré 1990). Operation of complexes III and I (sensitive to AA and Rtn, respectively) and mitochondrial MnSOD activity seem to be necessary for activation of aROS burst by flg22. Hence, during PTI, activation of MnSOD may help to scavenge the excess of O_2^- generated by mETC overloading and these changes may be required for optimal aROS generation.

In the mitochondrial compartment, ProDH can provide electrons to the ETC (Miller et al. 2009), apparently at the ubiquinone site (Schertl et al. 2014). ProDH contributes to generation of ROS in ETI and HR, and such ability was detected in gene silencing-based screens (Cecchini et al. 2011a; Senthil-Kumar and Mysore 2012). Here, we illustrate that ProDH also sustains flg22-induced responses relying on RBOHD activity, such as aROS generation, callose deposition, and *P. syringae* pv. *tomato-ΔhrcC* growth restriction (Fig. 2). So far, the plant ProDH has only been studied at the enzymatic level, with no other function being assigned to this protein. In contrast, bacterial ProDH (PutA) has two alternative functions, acting as transcriptional repressor or membrane-associated enzyme (Cecchini et al. 2011b; Szabados and Savouré 2010). In our system, the catalytic function of ProDH seems to be involved in activation of PTI, since the classical enzyme inhibitors T4C and THFA impair flg22-triggered aROS burst without being identified as NADPH

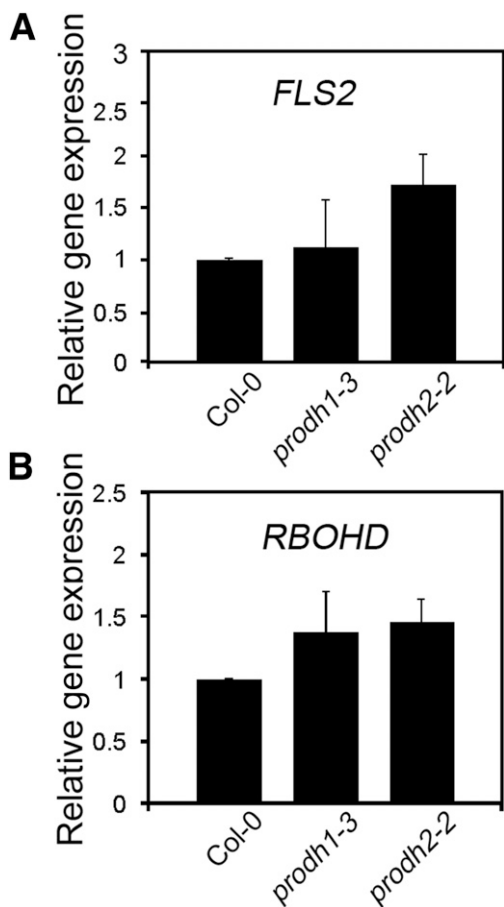


Fig. 3. Proline dehydrogenase (ProDH) mutants do not reduce *FLS2* and *RBOHD* expression. Quantitative polymerase chain reaction assays developed for **A**, *FLS2* and **B**, *RBOHD* in Col-0, *prodh1-3*, and *prodh2-2* samples. Values (mean \pm standard error of four biological assays) represent relative gene expression calculated by the Pfaffl method, using *UBQ5* as housekeeping gene. No significant differences were observed among samples (analysis of variance).

oxidase inhibitors in the numerous tests conducted by different research laboratories and pharmaceutical companies with this purpose (Cifuentes-Pagano et al. 2012).

Curiously, *prodh1-3* and *prodh2-2* mutants reduced PTI responses in a similar manner, indicating that both ProDH

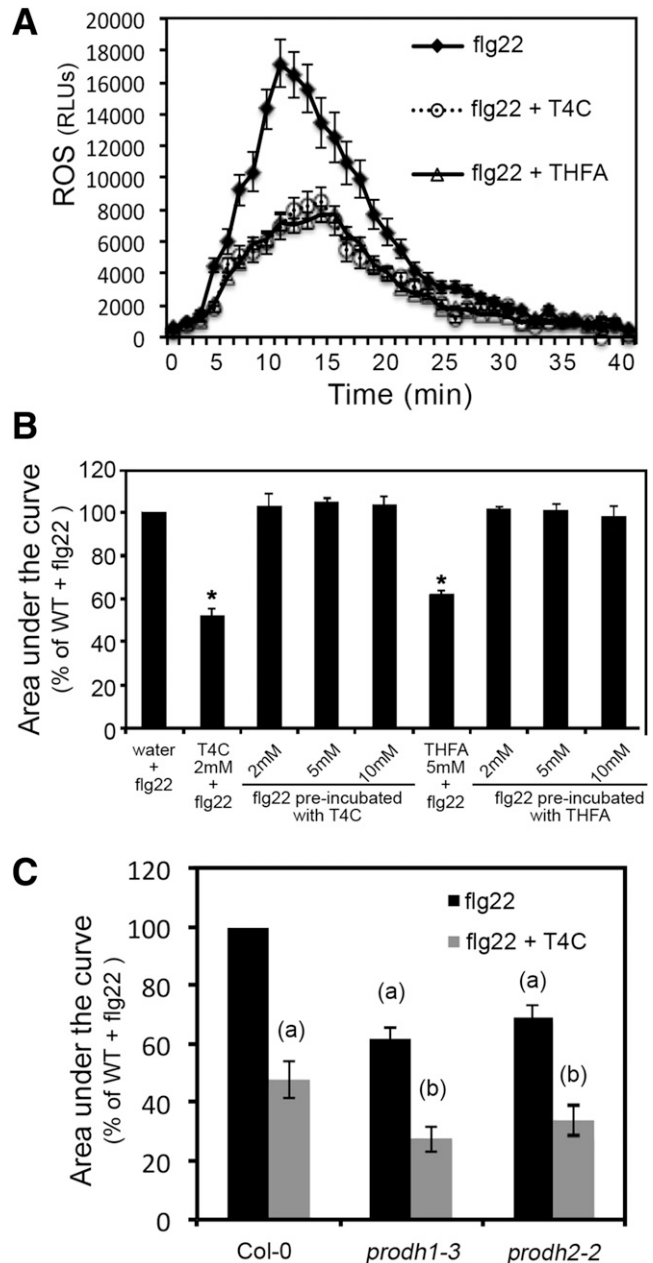


Fig. 4. Proline dehydrogenase (ProDH) activity influences flg22-induced apoplastic reactive oxygen species (ROS) burst. **A**, Time course of flg22-triggered ROS burst in Col-0 leaf discs pretreated (2 h) or not with the ProDH inhibitors thiazolidine-4-carboxylate (T4C) (2 mM) or L-tetrahydro-2-furoic acid (THFA) (5 mM). One representative experiment of three is shown. Values are mean \pm standard error (SE) of 24 discs per treatment. RLUs = relative luminescence units. **B**, flg22 (1 μ M) was coincubated with different concentrations of T4C or THFA for 2 h, was diluted 10 times, and then, was used to elicit ROS burst. Pretreatments (2 h) with T4C or THFA were used as controls. Values (mean \pm SE of three biological assays) represent percentage of water+flg22. Asterisks (*) indicate significant differences regarding preincubation with water (Z test $P < 0.05$). **C**, flg22-induced ROS levels in Col-0, *prodh1-3*, and *prodh2-2* pretreated (2 h) or not with T4C (2 mM). Values represent the average of three independent experiments expressed as mean \pm SE. Significant differences regarding Col-0+flg22 without (a) or with (b) T4C (Z test, $P < 0.05$).

isoforms contribute to this defense program. This contrasts with the notion of a leading role of *ProDH1* in tolerance to abiotic stress, manifested in studies with *prodh* single mutants (Funck et al. 2010; Sharma et al. 2011). Probably, ProDH1 and ProDH2 have cooperative effects, form heterodimers, or are otherwise interregulated. In bacteria, archaea, and eukaryotes such as *Trypanosoma cruzi* and humans, ProDH forms multimers (Kawakami et al. 2012; Lee et al. 2003; Paes et al. 2013; Tallarita et al. 2012; White et al. 2007), suggesting this could also occur with the plant enzyme.

Loss-of-function studies were complemented by application of exogenous Pro, which produces ProDH activation (Deuschle et al. 2001; Hellmann et al. 2000; Kiyosue et al. 1996). Pro (1 mM) treatment did not increase aROS by itself but potentiated flg22-induced aROS burst (Fig. 5B). In contrast to the first result, other authors reported that exogenous Pro was sufficient to produce ROS accumulation, likely by increasing cytosolic Ca^{2+} and, thus, enhancing NADPH oxidase activity (Chen et al. 2011). In this case, seedlings were exposed to high Pro (45 mM) for 24 h and ROS were detected by DAB staining, without evaluating their generation time. Probably, this RBOHD-dependent ROS burst may represent a late or secondary response derived from toxicity of high Pro doses (Deuschle et al. 2004). Alternatively, differences between results could be due to the large variations in Pro concentrations and exposure times used in both studies. In our system, exogenous Pro (1 mM) did not complement ROS deficiency of *prodh1-3* and *prodh2-2* plants exposed to flg22 (Fig. 5B), nor did this treatment apparently affect the generation of aROS by apoplastic peroxidases, since *rbohD* mutants treated with Pro and flg22 showed no ROS signal in the luminol assay (Fig. 5C) that was previously used to detect aROS burst triggered by fungal PAMPs (Bolwell et al. 2002). Based on these results, we suggest that 1 mM Pro potentiates flg22-induced aROS burst, dependent on RBOHD, by inducing ProDH activity.

The functional links between ProDH and RBOHD are still elusive. The different subcellular localization of these proteins precludes the notion of a direct interaction between them. In plants, humans, and insects, ProDH provides electrons to the mETC at ubiquinone (Goncalves et al. 2014; Phang et al. 2012; Schertl et al. 2014). Overstimulation of plant or animal ProDH generates mtROS under particular stress conditions (Miller et al. 2009; Phang et al. 2012). During PTI, ProDH could increase its activity and exacerbate the electron flow through the mETC. However, oxidation of Pro by ProDH does not appear to be sufficient to generate mtROS burst (Supplementary Fig. 3) (Miller et al. 2009). Therefore, for ProDH activity to affect mtROS levels, additional metabolic changes might be required. Eventually, mtROS may somehow signal aROS accumulation, as described for chloroplastic ROS (Zurbriggen et al. 2010).

On the other hand, ProDH may influence the balance of redox couples and, thus, affect the oxidative state of mitochondria, cytosol, or chloroplast (Ben Rejeb et al. 2014; Szabados and Savouré 2010). Plants impaired in a chloroplastic aspartate oxidase involved in NAD biosynthesis reduced flg22-induced ROS burst (Macho et al. 2012). Loss of the cytosolic NADP-malic enzyme 2 that may generate NADPH, diminished RBOHD-dependent aROS burst in response to flg22 and chitin (Voll et al. 2012). The increase in NAD(H) and NADP(H) levels by enhancement of NAD synthetase and NAD kinase activities improved resistance of rice plants to *Acidovorax avenae* (Hayashi et al. 2005). Curiously, at basal and stress conditions the *prodh1* mutant maintains the NAD/NADH balance and reduces the NADP/NADPH ratio, indicating a relative increase of NADPH (Sharma et al. 2011) that would not provide a direct explanation for low RBOHD activity in this plant. However, we cannot discard the possibility that particular imbalances of these couples

occurring at cytosol or organelles could influence this activity in *prodh* mutants. Eventually, ProDH could otherwise contribute to RBOHD function.

In summary, our work provides new insights regarding the interplay between mitochondria- and plasma membrane-based events during activation of plant innate immunity. Functional mETC and MnSOD as well as active ProDH are necessary to

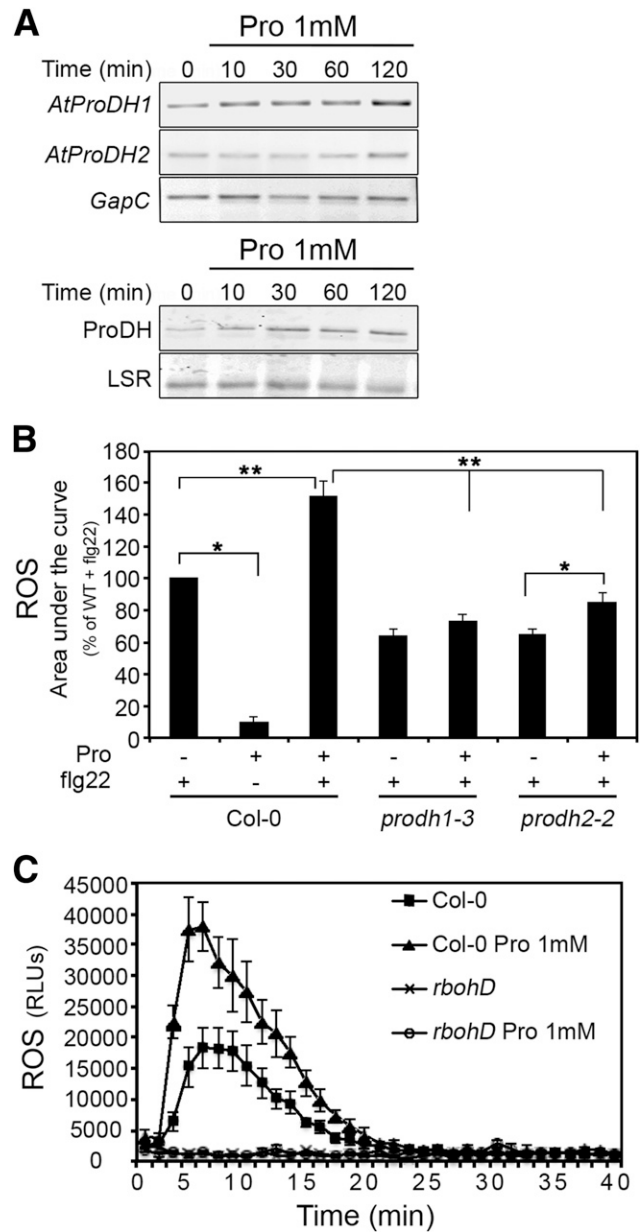


Fig. 5. Potentiation of flg22-induced apoplastic reactive oxygen species (ROS) by proline (Pro). **A**, Leaf discs were incubated with 1 mM Pro for the indicated times and were used to determine *AtProDH1* and *AtProDH2* transcripts (semiquantitative reverse transcription-polymerase chain reaction, top panel) or protein content (Western blot, bottom panel), using anti-Pro dehydrogenase (ProDH) antibodies that recognize both enzyme isoforms. LSR = large subunit of rubisco. **B**, Effect of Pro treatment (1 mM, 2 h) on subsequent ROS burst induced by flg22 in Col-0, *prodh1-3*, and *prodh2-2* plants. Values (average \pm standard error [SE] of three biological experiments, 24 leaf discs each). Asterisks (* and **) indicate significant differences at $P < 0.05$ or $P < 0.01$, respectively (Z test). **C**, Leaf discs of Col-0 and *rbohD* mutant plants were preincubated with Pro (1 mM, 2 h) before stimulation with flg22. One representative experiment of three biological replicates is shown. Points represent average \pm SE of 24 leaf discs. RLUs = relative luminescence units.

reach full expression of early and late PTI responses, with ProDH activity being required for maximal resistance to non-adapted pathogens and RBOHD-dependent ROS generation. These results provide key data to further investigate the precise mechanisms underlying the dialogue between ProDH and RBOHD.

MATERIALS AND METHODS

Plant growth and pathogen inoculation.

Arabidopsis Col-0 seeds were obtained from ABRC (*Arabidopsis* Biological Research Center, Columbus, OH, U.S.A.); *prodh1-3* (GABI_308F08), *prodh2-2* (GABI_328_G05), *prodh2-1* (GT1788), and Ler seeds were obtained from D. Funck (University of Konstanz, Germany) and *prodh1-4* (SALK_119334) from A. Savouré (Université Pierre-et-Marie-Curie, Paris); *rbohD* (Torres et al. 2005) and *fls2* (SALK_093905) were obtained from C. Zipfel (The Sainsbury Laboratory, Norwich, U.K.), MnSOD mutants (SALK_122275) from G. Pagnussat (University of Mar del Plata, Argentina) (Martin et al. 2013), and AS7 lines from L. Sweetlove (Morgan et al. 2008). Plant growth conditions are described elsewhere (Cambiagno et al. 2015). *P. syringae* pv. *tomato-ΔhrcC* was grown in solid King's B medium with rifampicin (100 µg/ml). Bacteria scraped from fresh plates were diluted and were used to spray leaves after the addition of Silwet L-77 (0.03% vol/vol). Pathogen growth was analyzed as described (Cambiagno et al. 2015), sampling by triplicate four leaf discs per genotype per time point.

Flg22-triggered aROS assay.

The flg22 peptide (QRLSTGSRINSKDDAAGLQIA) was synthesized by Pepton (Daejeon, South Korea) or the Institut de Biologie Integrative (The Centre National de la Recherche Scientifique, Paris) and was used at 100 nM. Leaf discs (0.38 cm²) were used to determine flg22-induced ROS levels by luminol assay (Gomez-Gomez et al. 1999) in a microplate reader (Synergy HT, Biotek, Winooski, VT, U.S.A.).

Treatments with inhibitors of mETC and ProDH.

AA (A8674, Sigma) was used at 10 µM and Rtn (Sigma, R8875) at 40 µM, diluted in water from ethanol stocks. These inhibitors were applied by floating leaf discs in water solutions or by spraying leaves with 0.03% (vol/vol) Silwet L-77. T4C (T27502, Sigma) and THFA (341517, Sigma) were applied at the indicated concentrations by floating leaf discs on the different solutions. T4C was diluted in water and THFA in Tris-buffer, pH 7.

Callose deposition and cell death.

Callose deposits were quantified in leaves infiltrated with of *P. syringae* pv. *tomato-ΔhrcC* (optical density at 600 nm = 0.005) or 100 nM flg22 at 16 h posttreatment, using aniline blue staining (Fabro et al. 2011). Samples were observed with an Axyoplan epifluorescence microscope (Carl Zeiss, Oberkochen, Germany) and images were taken with an Axiocam HRc (Carl Zeiss) to quantify callose dots with the ImageJ program. Cell death was determined with Sytox green (Cecchini et al. 2011a) on leaf discs pretreated with AA, Rtn, T4C, THFA, Pro, flg22, or *P. syringae* pv. *tomato AvrRPM1*. The number of nuclei per field was determined using ImageJ.

Semiquantitative reverse transcription-polymerase chain reaction (sqRT-PCR), quantitative (q)PCR, and Western blot.

sqRT-PCR and qRT-PCR were performed as described (Cambiagno et al. 2015; Rizzi et al. 2015). PCR conditions are indicated in Supplementary Table 1. Relative expression was calculated by the Pfaffl method: ratio between the efficiency

(E) of each target gene primer pair to the $-\Delta\Delta Ct^{(treated, basal)}$ and the E of *UBQ5* primer pair to the $-\Delta\Delta Ct^{(treated, basal)}$. Protein extraction, Western blot assay, and anti-ProDH antibodies are described in previous studies (Cecchini et al. 2011a, Monteoliva et al. 2014; Rizzi et al. 2015).

Subcellular localization of mitochondrial ROS.

ROS was detected by double-staining with 0.5 µM Mitotracker orange CMTMROS and 15 µM CM-H₂DCFDA (both from Thermo Fisher, Waltham, MA, U.S.A.). Whole leaves were syringe-infiltrated with AA (10 µM) or Rtn (40 µM), and then, with a mix of both fluorescent probes diluted in water. Leaf discs were observed with a laser-scanning confocal microscope (Olympus FV1000). Sequential images were acquired in green (CM-H₂DCFDA; excitation 488 nm, emission 510 to 530 nm) and red (Mitotracker orange; excitation 543 nm, emission, 560 to 600 nm) channels, using a 60× water objective with 1.4 NA.

ACKNOWLEDGMENTS

This work was supported by the Agencia Nacional de Promoción Científica y Tecnológica (PICT 2012-2117; PICT 2014-3255) and Secretaría de Ciencia y Tecnología Universidad Nacional de Córdoba granted to M. E. Alvarez, and by CONICET to G. Fabro. We thank C. Zipfel, D. Funck, A. Savouré, and G. Pagnussat for providing seeds. Y. S. Rizzi is a CONICET fellow and G. Fabro and M. E. Alvarez are senior career investigators of CONICET.

LITERATURE CITED

- Asai, T., Tena, G., Plotnikova, J., Willmann, M. R., Chiu, W. L., Gomez-Gomez, L., Boller, T., Ausubel, F. M., and Sheen, J. 2002. MAP kinase signalling cascade in *Arabidopsis* innate immunity. *Nature* 415:977-983.
- Ben Rejeb, K., Abdely, C., and Savouré, A. 2014. How reactive oxygen species and proline face stress together. *Plant Physiol. Biochem.* 80:278-284.
- Bolwell, G. P., Bindschedler, L. V., Blee, K. A., Butt, V. S., Davies, D. R., Gardner, S. L., Gerrish, C., and Minibayeva, F. 2002. The apoplastic oxidative burst in response to biotic stress in plants: A three-component system. *J. Exp. Bot.* 53:1367-1376.
- Boutrot, F., Segonzac, C., Chang, K. N., Qiao, H., Ecker, J. R., Zipfel, C., and Rathjen, J. P. 2010. Direct transcriptional control of the *Arabidopsis* immune receptor FLS2 by the ethylene-dependent transcription factors EIN3 and EIL1. *Proc. Natl. Acad. Sci. U.S.A.* 107:14502-14507.
- Brightman, A. O., and Morré, D. J. 1990. NADH oxidase of the plasma membrane of plants. Pages 85-110 in: *Oxidoreduction at the Plasma Membrane and its relation to Growth and Transport*. Vol. II. F. L. Crane, J. Morre, and H. E. Low, eds. CRC Press, Boca Raton, FL, U.S.A.
- Cambiagno, D. A., Loney, C., Ruyschaert, J. M., and Alvarez, M. E. 2015. The synthetic cationic lipid diC14 activates a sector of the *Arabidopsis* defence network requiring endogenous signalling components. *Mol. Plant Pathol.* 16:963-972.
- Cecchini, N. M., Monteoliva, M. I., Blanco, F., Holuigue, L., and Alvarez, M. E. 2009. Features of basal and race-specific defences in photosynthetic *Arabidopsis thaliana* suspension cultured cells. *Mol. Plant Pathol.* 10:305-310.
- Cecchini, N. M., Monteoliva, M. I., and Alvarez, M. E. 2011a. Proline dehydrogenase contributes to pathogen defense in *Arabidopsis*. *Plant Physiol.* 155:1947-1959.
- Cecchini, N. M., Monteoliva, M. I., and Alvarez, M. E. 2011b. Proline dehydrogenase is a positive regulator of cell death in different kingdoms. *Plant Signal. Behav.* 6:1195-1197.
- Cecchini, N. M., Jung, H. W., Engle, N. L., Tschaplinski, T. J., and Greenberg, J. T. 2015. ALD1 regulates basal immune components and early inducible defense responses in *Arabidopsis*. *Mol. Plant-Microbe Interact.* 28:455-466.
- Chaouch, S., Queval, G., and Noctor, G. 2012. AtRbohF is a crucial modulator of defence-associated metabolism and a key actor in the interplay between intracellular oxidative stress and pathogenesis responses in *Arabidopsis*. *Plant J.* 69:613-627.
- Chen, J., Zhang, Y., Wang, C., Lu, W., Jin, J. B., and Hua, X. 2011. Proline induces calcium-mediated oxidative burst and salicylic acid signaling. *Amino Acids* 40:1473-1484.
- Cifuentes-Pagano, E., Csanyi, G., and Pagano, P. J. 2012. NADPH oxidase inhibitors: A decade of discovery from Nox2ds to HTS. *Cell. Mol. Life Sci.* 69:2315-2325.

- Cvetkovska, M., and Vanlerberghe, G. C. 2012. Coordination of a mitochondrial superoxide burst during the hypersensitive response to bacterial pathogen in *Nicotiana tabacum*. *Plant Cell Environ.* 35:1121-1136.
- Daudi, A., Cheng, Z., O'Brien, J. A., Mammarella, N., Khan, S., Ausubel, F. M., and Bolwell, G. P. 2012. The apoplastic oxidative burst peroxidase in *Arabidopsis* is a major component of pattern-triggered immunity. *Plant Cell* 24:275-287.
- Deuschle, K., Funck, D., Hellmann, H., Daschner, K., Binder, S., and Frommer, W. B. 2001. A nuclear gene encoding mitochondrial Δ^1 -pyrroline-5-carboxylate dehydrogenase and its potential role in protection from proline toxicity. *Plant J.* 27:345-356.
- Deuschle, K., Funck, D., Forlani, G., Stransky, H., Biehl, A., Leister, D., van der Graaff, E., Kunze, R., and Frommer, W. B. 2004. The role of Δ^1 -pyrroline-5-carboxylate dehydrogenase in proline degradation. *Plant Cell* 16:3413-3425.
- Elthon, T. E., and Stewart, C. R. 1981. Submitochondrial location and electron transport characteristics of enzymes involved in proline oxidation. *Plant Physiol.* 67:780-784.
- Elthon, T. E., and Stewart, C. R. 1984. Effects of the proline analog l-thiazolidine-4-carboxylic acid on proline metabolism. *Plant Physiol.* 74:213-218.
- Fabro, G., Steinbrenner, J., Coates, M., Ishaque, N., Baxter, L., Studholme, D. J., Korner, E., Allen, R. L., Piquerez, S. J., Rougon-Cardoso, A., Greenshields, D., Lei, R., Badel, J. L., Caillaud, M. C., Sohn, K. H., Van den Ackerveken, G., Parker, J. E., Beynon, J., and Jones, J. D. 2011. Multiple candidate effectors from the oomycete pathogen *Hyaloperonospora arabidopsidis* suppress host plant immunity. *PLoS Pathog.* 7: e1002348.
- Funck, D., Eckard, S., and Muller, G. 2010. Non-redundant functions of two proline dehydrogenase isoforms in Arabidopsis. *BMC Plant Biol.* 10:70.
- Galletti, R., Denoux, C., Gambetta, S., Dewdney, J., Ausubel, F. M., De Lorenzo, G., and Ferrari, S. 2008. The AtrbohD-mediated oxidative burst elicited by oligogalacturonides in Arabidopsis is dispensable for the activation of defense responses effective against *Botrytis cinerea*. *Plant Physiol.* 148:1695-1706.
- Gleason, C., Huang, S., Thatcher, L. F., Foley, R. C., Anderson, C. R., Carroll, A. J., Millar, A. H., and Singh, K. B. 2011. Mitochondrial complex II has a key role in mitochondrial-derived reactive oxygen species influence on plant stress gene regulation and defense. *Proc. Natl. Acad. Sci. U.S.A.* 108:10768-10773.
- Gómez-Gómez, L., Felix, G., and Boller, T. 1999. A single locus determines sensitivity to bacterial flagellin in *Arabidopsis thaliana*. *Plant J.* 18: 277-284.
- Goncalves, R. L., Rothschild, D. E., Quinlan, C. L., Scott, G. K., Benz, C. C., and Brand, M. D. 2014. Sources of superoxide/H₂O₂ during mitochondrial proline oxidation. *Redox Biol.* 2:901-909.
- Hayashi, M., Takahashi, H., Tamura, K., Huang, J., Yu, L. H., Kawai-Yamada, M., Tezuka, T., and Uchimiya, H. 2005. Enhanced dihydroflavonol-4-reductase activity and NAD homeostasis leading to cell death tolerance in transgenic rice. *Proc. Natl. Acad. Sci. U.S.A.* 102: 7020-7025.
- Hellmann, H., Funck, D., Rentsch, D., and Frommer, W. B. 2000. Hypersensitivity of an Arabidopsis sugar signaling mutant toward exogenous proline application. *Plant Physiol.* 123:779-789.
- Huang, Y., Chen, X., Liu, Y., Roth, C., Copeland, C., McFarlane, H. E., Huang, S., Lipka, V., Wiermer, M., and Li, X. 2013. Mitochondrial AtPAM16 is required for plant survival and the negative regulation of plant immunity. *Nat. Commun.* 4:2558.
- Kadota, Y., Shirasu, K., and Zipfel, C. 2015. Regulation of the NADPH oxidase RBOHD during plant immunity. *Plant Cell Physiol.* 56:1472-1480.
- Kawakami, R., Satomura, T., Sakuraba, H., and Ohshima, T. 2012. L-proline dehydrogenases in hyperthermophilic archaea: Distribution, function, structure, and application. *Appl. Microbiol. Biotechnol.* 93: 83-93.
- Kiyosue, T., Yoshida, Y., Yamaguchi-Shinozaki, K., and Shinozaki, K. 1996. A nuclear gene encoding mitochondrial proline dehydrogenase, an enzyme involved in proline metabolism, is upregulated by proline but downregulated by dehydration in Arabidopsis. *Plant Cell* 8:1323-1335.
- Krause, M., and Durner, J. 2004. Harpin inactivates mitochondria in *Arabidopsis* suspension cells. *Mol. Plant-Microbe Interact.* 17:131-139.
- Krishnan, N., Dickman, M. B., and Becker, D. F. 2008. Proline modulates the intracellular redox environment and protects mammalian cells against oxidative stress. *Free Radic. Biol. Med.* 44:671-681.
- Lam, E., Kato, N., and Lawton, M. 2001. Programmed cell death, mitochondria and the plant hypersensitive response. *Nature* 411:848-853.
- Lee, Y. H., Nadarai, S., Gu, D., Becker, D. F., and Tanner, J. J. 2003. Structure of the proline dehydrogenase domain of the multifunctional PutA flavoprotein. *Nat. Struct. Biol.* 10:109-114.
- Macho, A. P., Boutrot, F., Rathjen, J. P., and Zipfel, C. 2012. Aspartate oxidase plays an important role in Arabidopsis stomatal immunity. *Plant Physiol.* 159:1845-1856.
- Martin, M. V., Fiol, D. F., Sundaresan, V., Zabaleta, E. J., and Pagnussat, G. C. 2013. *oiwa*, a female gametophytic mutant impaired in a mitochondrial manganese-superoxide dismutase, reveals crucial roles for reactive oxygen species during embryo sac development and fertilization in *Arabidopsis*. *Plant Cell* 25:1573-1591.
- Mersmann, S., Bourdais, G., Rietz, S., and Robatzek, S. 2010. Ethylene signaling regulates accumulation of the FLS2 receptor and is required for the oxidative burst contributing to plant immunity. *Plant Physiol.* 154: 391-400.
- Miller, G., Honig, A., Stein, H., Suzuki, N., Mittler, R., and Zilberstein, A. 2009. Unraveling Δ^1 -pyrroline-5-carboxylate-proline cycle in plants by uncoupled expression of proline oxidation enzymes. *J. Biol. Chem.* 284: 26482-26492.
- Møller, I. M. 2001. Plant mitochondria and oxidative stress: Electron transport, NADPH Turnover, and metabolism of reactive oxygen species. *Annu. Rev. Plant Physiol. Plant Mol. Biol.* 52:561-591.
- Monaghan, J., Matschi, S., Shorinola, O., Rovenich, H., Matei, A., Segonzac, C., Malinovsky, F. G., Rathjen, J. P., MacLean, D., Romeis, T., and Zipfel, C. 2014. The calcium-dependent protein kinase CPK28 buffers plant immunity and regulates BIK1 turnover. *Cell Host Microbe* 16:605-615.
- Monteoliva, M. I., Rizzi, Y. S., Cecchini, N. M., Hajirezaei, M. R., and Alvarez, M. E. 2014. Context of action of proline dehydrogenase (ProDH) in the hypersensitive response of Arabidopsis. *BMC Plant Biol.* 14:21.
- Morgan, M. J., Lehmann, M., Schwarzlander, M., Baxter, C. J., Sienkiewicz-Portucek, A., Williams, T. C., Schauer, N., Fernie, A. R., Fricker, M. D., Ratcliffe, R. G., Sweetlove, L. J., and Finkemeier, I. 2008. Decrease in manganese superoxide dismutase leads to reduced root growth and affects tricarboxylic acid cycle flux and mitochondrial redox homeostasis. *Plant Physiol.* 147:101-114.
- Mur, L. A., Kenton, P., Lloyd, A. J., Ougham, H., and Prats, E. 2008. The hypersensitive response; the centenary is upon us but how much do we know? *J. Exp. Bot.* 59:501-520.
- Nicaise, V., Roux, M., and Zipfel, C. 2009. Recent advances in PAMP-triggered immunity against bacteria: Pattern recognition receptors watch over and raise the alarm. *Plant Physiol.* 150:1638-1647.
- Norman, C., Howell, K. A., Millar, A. H., Whelan, J. M., and Day, D. A. 2004. Salicylic acid is an uncoupler and inhibitor of mitochondrial electron transport. *Plant Physiol.* 134:492-501.
- Paes, L. S., Suarez Mantilla, B., Zimbres, F. M., Pral, E. M., Diogo de Melo, P., Tahara, E. B., Kowaltowski, A. J., Elias, M. C., and Silber, A. M. 2013. Proline dehydrogenase regulates redox state and respiratory metabolism in *Trypanosoma cruzi*. *PLoS One* 8:e69419.
- Pandey, S. P., and Somssich, I. E. 2009. The role of WRKY transcription factors in plant immunity. *Plant Physiol.* 150:1648-1655.
- Phang, J. M., Liu, W., Hancock, C., and Christian, K. J. 2012. The proline regulatory axis and cancer. *Front. Oncol.* 2:60.
- Rizzi, Y. S., Monteoliva, M. I., Fabro, G., Grosso, C. L., Larovere, L. E., and Alvarez, M. E. 2015. P5CDH affects the pathways contributing to Pro synthesis after ProDH activation by biotic and abiotic stress conditions. *Front. Plant Sci.* 6:572.
- Schertl, P., Cabassa, C., Saadallah, K., Bordenave, M., Savouré, A., and Braun, H. P. 2014. Biochemical characterization of proline dehydrogenase in Arabidopsis mitochondria. *FEBS J.* 281:2794-2804.
- Senthil-Kumar, M., and Mysore, K. S. 2012. Ornithine-delta-aminotransferase and proline dehydrogenase genes play a role in non-host disease resistance by regulating pyrroline-5-carboxylate metabolism-induced hypersensitive response. *Plant Cell Environ.* 35:1329-1343.
- Shapiguzov, A., Vainonen, J. P., Wrzaczek, M., and Kangasjarvi, J. 2012. ROS-talk—How the apoplast, the chloroplast, and the nucleus get the message through. *Front. Plant Sci.* 3:292.
- Sharma, S., Villamor, J. G., and Verslues, P. E. 2011. Essential role of tissue-specific proline synthesis and catabolism in growth and redox balance at low water potential. *Plant Physiol.* 157:292-304.
- Stegmann, M., Anderson, R. G., Ichimura, K., Pecenkova, T., Reuter, P., Zarsky, V., McDowell, J. M., Shirasu, K., and Trujillo, M. 2012. The ubiquitin ligase PUB22 targets a subunit of the exocyst complex required for PAMP-triggered responses in *Arabidopsis*. *Plant Cell* 24: 4703-4716.
- Szabados, L., and Savouré, A. 2010. Proline: A multifunctional amino acid. *Trends Plant Sci.* 15:89-97.
- Tallarita, E., Pollegioni, L., Servi, S., and Molla, G. 2012. Expression in *Escherichia coli* of the catalytic domain of human proline oxidase. *Protein Expr. Purif.* 82:345-351.

- Torres, M. A., Jones, J. D., and Dangl, J. L. 2005. Pathogen-induced, NADPH oxidase-derived reactive oxygen intermediates suppress spread of cell death in *Arabidopsis thaliana*. *Nat. Genet.* 37:1130-1134.
- Tsuda, K., and Katagiri, F. 2010. Comparing signaling mechanisms engaged in pattern-triggered and effector-triggered immunity. *Curr. Opin. Plant Biol.* 13:459-465.
- Voll, L. M., Zell, M. B., Engelsdorf, T., Saur, A., Wheeler, M. G., Drincovich, M. F., Weber, A. P. M., and Maurino, V. G. 2012. Loss of cytosolic NADP-malic enzyme 2 in *Arabidopsis thaliana* is associated with enhanced susceptibility to *Colletotrichum higginsianum*. *New Phytol.* 195:189-202.
- White, T. A., Krishnan, N., Becker, D. F., and Tanner, J. J. 2007. Structure and kinetics of monofunctional proline dehydrogenase from *Thermus thermophilus*. *J. Biol. Chem.* 282:14316-14327.
- Xie, Z., and Chen, Z. 1999. Salicylic acid induces rapid inhibition of mitochondrial electron transport and oxidative phosphorylation in tobacco cells. *Plant Physiol.* 120:217-226.
- Xie, Z., and Chen, Z. 2000. Harpin-induced hypersensitive cell death is associated with altered mitochondrial functions in tobacco cells. *Mol. Plant-Microbe Interact.* 13:183-190.
- Yao, N., and Greenberg, J. T. 2006. *Arabidopsis* ACCELERATED CELL DEATH2 modulates programmed cell death. *Plant Cell* 18:397-411.
- Yi, S. Y., Shirasu, K., Moon, J. S., Lee, S. G., and Kwon, S. Y. 2014. The activated SA and JA signaling pathways have an influence on flg22-triggered oxidative burst and callose deposition. *PLoS One* 9:e88951.
- Zhang, L., and Xing, D. 2008. Methyl jasmonate induces production of reactive oxygen species and alterations in mitochondrial dynamics that precede photosynthetic dysfunction and subsequent cell death. *Plant Cell Physiol.* 49:1092-1111.
- Zhang, B., Van Aken, O., Thatcher, L., De Clercq, I., Duncan, O., Law, S. R., Murcha, M. W., van der Merwe, M., Seifi, H. S., Carrie, C., Cazzonelli, C., Radomiljac, J., Hofte, M., Singh, K. B., Van Breusegem, F., and Whelan, J. 2014. The mitochondrial outer membrane AAA ATPase AtOM66 affects cell death and pathogen resistance in *Arabidopsis thaliana*. *Plant J.* 80:709-727.
- Zhu, W., Gincherman, Y., Docherty, P., Spilling, C. D., and Becker, D. F. 2002. Effects of proline analog binding on the spectroscopic and redox properties of PutA. *Arch. Biochem. Biophys.* 408:131-136.
- Zipfel, C., Robatzek, S., Navarro, L., Oakeley, E. J., Jones, J. D., Felix, G., and Boller, T. 2004. Bacterial disease resistance in *Arabidopsis* through flagellin perception. *Nature* 428:764-767.
- Zurbriggen, M. D., Carrillo, N., and Hajirezaei, M. R. 2010. ROS signaling in the hypersensitive response: When, where and what for? *Plant Signal. Behav.* 5:393-396.